Three Types of Isocoumarins with Unusual Carbon Skeletons from Artemisia dubia var. subdigitata and Their Antihepatoma Activity

Ke-Xin Yang[1], Tian-Ze Li[1], Yun-Bao Ma[1], Yong-Cui Wang[1], Feng-Jiao Li[1], and Jijun Chen[1]

[1]Kunming Institute of Botany Chinese Academy of Sciences

April 30, 2024

Abstract

Ten novel isocoumarins, including four pairs of enantiomers, were isolated from Artemisia dubia var. subdigitata (Asteraceae). Com-pounds 1, 2 and 3a/3b possessed a unique 6/6/6-tricyclic system comprising an unusual 1-(2-methylcyclohexyl) propan-1-one moiety fused with isocoumarin core skeleton. Compounds 4a/4b were characterized as an unexpected 2,5-dimethylcyclohexan-1-one scaffold, and compounds 5a/5b and 6a/6b were rare 1,2-seco-isocoumarin. Their structures and absolute configurations were elucidated through spectroscopic data, X-ray crystallography, ECD and NMR calculations with DP4+ analyses. Plausible biosynthetic pathways were proposed from the naturally occurring isocoumarin. Network pharmacological analysis suggested that the targets of compound 1 were significantly enriched in the cell cycle and PI3K-Akt signaling pathway. The molecular docking revealed that compound 1 had high binding affinity with CDK2 (total score: 6.8717). Furthermore, compounds 1 and 2 exhibited inhibitory activity on three human hepa-toma cell lines, with inhibitory ratios of 85.1% and 84.5% (HepG2), 88.2% and 87.3% (Huh7), and 69.2% and 69.1% (SK-Hep-1) at 200 μM, respectively.

Cite this paper:*Chin. J. Chem.* **2024** , *42* , XXX—XXX. **DOI: 10.1002/cjoc.202400XXX**

Three Types of Isocoumarins with Unusual Carbon Skeletons from*Artemisia dubia* var. *subdigitata* and Their Antihepatoma Activity

Ke-Xin Yang,[a,b] Tian-Ze Li,[a] Yun-Bao Ma,[a]Yong-Cui Wang,[a] Feng-Jiao Li,[a,b] and Ji-Jun Chen *[,a,b]

[a] State Key Laboratory of Phytochemistry and Plant Resources in West China, Kunming Institute of Botany, Chinese Academy of Sciences, Kunming 650201, People's Republic of China[b] University of Chinese Academy of Sciences, Beijing 100049, People's Republic of China

Keywords

Artemisia dubia var. *subdigitata* | Artemdubones A-F | Isocoumarins | Antihepatoma activity | CDK2

Comprehensive Summary

Ten novel isocoumarins, including four pairs of enantiomers, were isolated from *Artemisia dubia* var. *subdigitata* (Asteracea

Background and Originality Content

Liver cancer remains a significant global health challenge with an estimated incidence of over one million cases by 2025.[1-2] Hepatocellular carcinoma (HCC) represents the predominant type of liver cancer, constituting approximately 90% of all cases,[3] and characterized by a high degree of malignancy and a poor treatment outcome, which is difficult to diagnose in its early stage. It was reported that molecular signaling pathway was identified as one of the main mechanisms of HCC progression.[4] Currently, five small molecule kinase inhibitors (sorafenib, lenvatinib, regorafenib, cabozantinib, and donafenib), and three antibody drugs (nivolumab, pembrolizumab, and ramucirumab) have improved the overall survival rate of HCC patients.[5] However, these drugs face short-term effectiveness and drug resistance due to their similar structures and target mechanisms. Therefore, there is an urgent need to discover new agents that possess different structure and novel molecular mechanism to overcome drug resistance.

The structural diversities of natural products play an important role in drug discovery.[6] Isocoumarins, as the isomers of coumarins with an inverted lactone ring, are abundant in fungi, bacteria, and terrestrial plants.[7] Up to now, nearly one thousand isocoumarins had been isolated, including a total of 351 structurally diverse ones from fungi in the past twenty years.[8-9] Isocoumarins displayed a wide range of biological activities, such as antifungal, antimicrobial, anticancer, antidiabetic, and anti-inflammatory effects.[10-13] The genus *Artemisia* , one of the largest genera within the family Asteraceae, comprises about 380 species worldwide.[14] Certain species of this genus have been traditionally used as a folk medicine in China. For example, *A. annua* has been used for the treatment of intermittent fevers since ancient times, and its main component, artemisinin, has excellent anti-malarial activity.[15] *Artemisia* plants have a diverse range of chemical components, including sesquiterpenoids and their dimers, flavonoids, lignans, and coumarins. [16-17] However, there have been fewer reports on isocoumarins from the genus *Artemisia* , and only ten compounds were reported to date.[18-21] In addition, there is no research available regarding the activity of isocoumarins against HCC within the genus *Artemisia* .

A. dubia var. *subdigitata* is considered as a variety of *A. dubia* , and has been used as a folk medicine to treat lung-heat cough, swollen sore throat, acute calenture, and rubella.[22] However, neither the constituents nor the antihepatoma activity of *A. dubia* var. *subdigitata* has been reported. To search for structurally novel and bioactive constituents, artemdubones A-F, including four pairs of enantiomers, were isolated, and their structures were elucidated by extensive spectral data, ECD and NMR calculations, X-ray crystallography. Interestingly, compounds **1** , **2** , and **3a/3b**possessed a unique 6/6/6-tricyclic system composing an unprecedented 1-(2-methylcyclohexyl) propan-1-one moiety and isocoumarin core skeleton. Compounds **4a/4b** incorporated an unexpected 2,5-dimethylcyclohexan-1-one scaffold, and compounds **5a/5b** and**6a/6b** featured a rare 1,2-*seco* -isocoumarin. Furthermore, we utilized network pharmacology and molecular docking to investigate the potential targets and mechanisms of compound **1** . The analysis suggested that the targets of compound **1** were significantly enriched in the cell cycle and PI3K-Akt signaling pathway, with CDK2 identified as a potential target protein. In order to further validate the antihepatoma activities, the obtained compounds**1** -**6** were evaluated on three human hepatoma cell lines, and the results showed compounds **1** and **2** exhibited inhibitory activity on three cell lines with inhibitory ratios of 85.1% and 84.5% (HepG2), 88.2% and 87.3% (Huh7), and 69.2% and 69.1% (SK-Hep-1) at 200 μ M, respectively. Herein, we described the isolation, structural elucidation, plausible biosynthetic pathways, and antihepatoma activities on HepG2, Huh7, and SK-Hep-1 cell lines.

Figure 1 Chemical structures of artemdubones A-F (**1** -**6**).

Results and Discussion

Artemdubone A (**1**), white triclinic crystals, had a molecular formula of $C_{17}H_{18}O_4$ as determined by its (–)-HRESIMS (*m/z* : 285.1162 $[M - H]^-$, calcd for $C_{17}H_{17}O_4$, 285.1149), requiring nine double bond equivalents (DBEs). The IR absorptions at 3445, 1716, and 1656 cm^{-1} exhibited the presence of hydroxy, carbonyl, and double bond groups. The ^1H NMR spectrum of compound **1** (Table 1) revealed four aromatic proton signals [δ_H 7.58 (m); 7.87 (m); 7.90 (br d, J = 7.5 Hz); 8.23 (br d, J = 7.9 Hz)], one oxymethine proton (δ_H 5.08, br s), and two methyl groups [(δ_H1.06 (t, J = 7.2 Hz); 1.12 (d, J = 7.1 Hz)]. Analysis of the ^{13}C NMR (DEPT) spectra (Table 2) exhibited a total of 17 carbon resonances divided into two methyl groups, two

methylenes, seven methines, and six quaternary carbons. The ^{1}H–^{1}H COSY spectrum (Figure 2) revealed a spin coupling system of H-5/H-6/H-7/H-8. The HMBC correlations (Figure 2) from H-5 to C-4/C-7, and from H-8 to C-1/C-6 suggested the presence of isocoumarin core skeleton in **1** (A and B rings).[23] Apart from the isocoumarin moiety, a carbonyl group accounted for one degree of unsaturation, and the remained one degree of unsaturation indicated the presence of an additional ring. The proton spin systems of H-1'/H_2-2'/H-3'/H-4' and H_2-6'/H_3-7' in the^{1}H–^{1}H COSY spectrum and the correlations from H-8' to C-2'/C-3'/C-4', and from H-6' to C-4'/C-5' in the HMBC spectrum led to the assignment of a 1'-hydroxy-3'-methylheptan-5'-one moiety. Furthermore, the HMBC correlations from H-1' and H-4' to C-3/C-4, and from H-2' to C-4 revealed the connections of C-1'–C-4 and C-4'–C-3 bonds to form a hexane ring (ring C). Thus, the planar structure of **1** was assigned with a 6/6/6 tricyclic skeleton (Figure 1).

The relative configuration of compound **1** was determined by the interpretation of coupling constants (J) and the ROESY correlations. The small coupling constant of H-4' with H-3' ($J_{\text{H-3'/H-4'}} = 6.2$ Hz) indicated the same orientation of H-3' and H-4'. However, it was difficult to identify the configuration of C-1' by ROESY experiments. A single crystal was successfully obtained and a X-ray crystallographic analysis was performed using anomalous dispersion with copper radiation (Figure 5), which determined its absolute configuration as 1'S ,3'S ,4'S [flack parameter = 0.22(17)].

Artemdubone B (**2**) was obtained as white powers and had the same molecular formula $C_{17}H_{18}O_4$ as **1**based on the (+)-HRESIMS spectrum (m/z 287.1266 $[M + H]^+$, calcd for $C_{17}H_{19}O_4$, 287.1278). Detailed analyses of their 1D and 2D NMR data revealed compound**2** was an epimer of **1** at C-4'. The large coupling constant between H-3' and H-4' (10.5 Hz) suggested their *trans*arrangements. The correlation of H-4' with H_3-8' in the ROESY spectrum (Figure 3) further verified the aboved inference. Thus, the remained two reasonable diastereoisomers, (1'S *,3'S *,4'R *) **-2** , (1'R *,3'S *,4'R *) **-2,** were performed using quantum chemical calculation of NMR chemical shifts at Mpw1pw91/ 6-31+G (d,p) level. Analyses of the results were undertaken on correlation coefficient (R^2), mean absolute error (MAE), corrected mean absolute error (CMAE), and DP4+ probability of each candidate.[24] As a result (Figure 4), the calculated ^{13}C NMR chemical shifts of (1'S *,3'S *,4'R *) **-2** were in good agreement with the experimental data with a high R^2 of 0.9981, and a low MAE and CMAE of 2.4 and 2.4 ppm, respectively. In addition, the DP4+ probability also showed (1'S *,3'S *,4'R *) **-2** might be the real structure with 100% $DP4^+$ probability (all data). Based on the above evidence, the relative configuration of **2**was determined. Therefore, the absolute configuration of compound**2** was assigned as 1'S ,3'S ,4'R by comparison of the experimental and calculated ECD spectra (Figure 6).

Figure 2 Key ^{1}H-^{1}H COSY and HMBC correlations of compounds **1** -**6** .

Figure 3 Key ROESY correlations of compounds**1** -**6** .

Artemdubone C (**3**) possessed the same molecular formula as compound **2** by their HRESIMS data. The NMR data (Tables 1 and 2) of compound **3** resembled those of **2** , and the major differences were chemical shifts of C-2' (δ_C39.5, $\Delta\delta_C$ 0.7), C-3' (δ_C31.4, $\Delta\delta_C$ 2.8), C-4' (δ_C59.4, $\Delta\delta_C$ 1.3), implying the different orientation of methyl group at C-3'. This difference was verified by the ROESY correlations of H-1'/H-3' (Figure 3), and the small coupling constant of H-4' with H-3' ($J_{\text{H-3'/H-4'}} = 7.0$ Hz). Interestingly, compound **3** was a pair of enantiomers, which was estabilished based on the small optical rotations. Subsequent chiral HPLC separation afforded enantiomers **3a** and **3b** . Their absolute configurations were defined as 1'S ,3'R ,4'R(**3a**) and 1'R ,3'S ,4'S (**3b**) by comparison of the computational and experimental ECD data (Figure 6).

Artemdubone D (**4**) was obtained as colorless triclinic crystals from MeOH and gave a molecular formula of $C_{17}H_{18}O_4$ from the (+)-HRESIMS ion at m/z 287.1262 $[M + H]^+$(calcd for $C_{17}H_{19}O_4$, 287.1278). The ^{1}H and ^{13}C NMR data (Tables 1 and 2) indicated that compound **4** was closely related to **1** , but the major differences were the signals for ring C. The ^{1}H–^{1}H COSY correlation (Figure 2) of H-6'/H-1'/H-2'/H-3'/H-4', together with the HMBC correlations (Figure 2) from H_3-8' to C-2'/C-3'/C-4' and from H_3-7' to C-1'/C-5'/C-6' revealed the presence of a 1'-hydroxy-3', 6'-dimethylcyclohexan-5'-one scaffold (ring C).

Ring C linking to the ring B through C-3–C-4' bond was comprised by the HMBC correlations from H-4' to C-3/C-4. The *trans* -axial orientations of H-3' and H-4' were established based on the large couping constant ($J_{3',4'}$ = 12.1 Hz).The ROESY correlations (Figure 3) of H-4'/H_3-8', H-1'/H-3', and H-1'/H_3-7' indicated the cofacial orientation of these protons. To definitively determine this unprecedented structure and absolute configuration, a single crystal was obtained. The X-ray data (Figure 5) revealed that **4** possessed a centrosymmetric space group $P\ 121/c\ 1$, showing recemic nature.[25] An HPLC analysis was carried out using a chiral column to obtain compounds **4a** and **4b** . The absolute configurations of **4a** and **4b** were assigned as 1'*R* ,3'*S* ,4'*S* ,6'*S* , and 1'*S* ,3'*R* ,4'*R* ,6'*R* , by comparision of experimental and calculated ECD spectra, respectively.

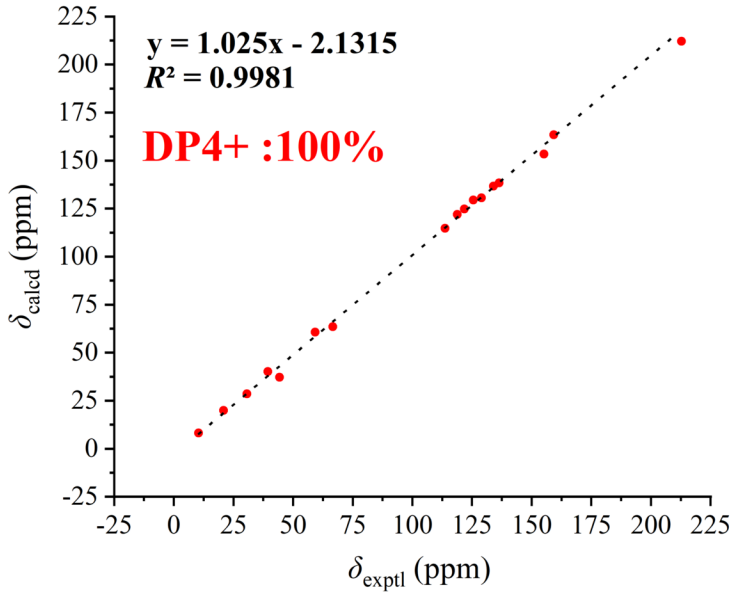

Figure 4 Correlation plots of experimental and^{13}C NMR spectral data for (1'*S* *, 3'*S* *, 4'*R* *) **-2** and DP4+ results.

Figure 5 The X-ray ORTEP drawings of compounds **1** and**4a** /**4b** .

Artemdubone E (**5**) possessed a molecular formula $C_{19}H_{24}O_5$ as assigned by the (+)-HRESIMS ion at *m/z* 355.1524 $[M + Na]^+$ (calculated for $C_{19}H_{24}O_5Na$, 355.1516). The ^{13}C NMR (DEPT) spectrum of **5** (Table 2) revealed the existence of two carbonyl groups (δ_C208.5 and 204.4), one ester-carbonyl group (δ_C167.2). The NMR data indicated that compound **5** had similar structure with **4** except for the signals for ring B. The^{1}H–^{1}H COSY correlation (Figure 2) of H-1"/H-2", as well as the HMBC correlations (Figure 2) from H_2-4 to C-3/C-9, and from H-1" to C-1, suggested that the rupture of the lactone ring (B ring), followed by the ethoxy group at the C-1 position and the carbonyl group at the C-3 position in**5** . The large couping constant of H-3' and H-4' ($J_{3',4'}$ = 11.8 Hz) indicated their*trans* -diaxial orientation. The ROESY correlations (Figure 3) of H-4'/H_3-8' and H_3-7'/H-1'/H-3' explained the β -orientation of H-1', H-3', and H_3-7', theα -orientation of H-4' and H_3-8'. Interestingly, compound **5** was found to consist of a pair of enantiomers by the lack of any Cotton effect in the ECD spectrum. Subsequent HPLC separation afforded enantiomers **5a** and **5b** and their absolute configurations were clarified as 1'*R* ,3'*S* ,4'*S* ,6'*S* and 1'*S* ,3'*R* ,4'*R* ,6'*R* by comparison of the experimental and calculated ECD spectra, respectively.

Artemdubone F (**6**) had the same molecular formula of $C_{19}H_{24}O_5$ as compound**5** . The 1D NMR (Tables

1 and 2) spectra of compounds **6**and **5** were similar, and the major differences were chemical shifts of C-1' (δ_C 74.1 *vs* 73.7), C-2' (δ_C 42.4 *vs* 40.4), and C-6' (δ_C 53.9 *vs* 49.8), H-1' (δ_H 3.46 *vs* 3.37), H-2' (δ_H 2.18, 1.56 *vs* 2.10, 1.72), and H-6' (δ_H 2.41 *vs* 2.84). Detailed analyses of 2D NMR data demonstrated that compound **6** was an epimer of**5** at C-1', which was corroborated by the key ROESY correlation of H_3-8'/H-4'/H-6'/H-1'. The optical rotation value of**6** was close to zero,

Table 1 ^{1}H NMR data (600 MHz) for compounds**1** -**6** (δ in ppm, J in Hz).

No.	**1**[a]	**2**[a]	**3a/3b**[a]	**4a/4b**[b]	**5a/5b**[b]	**6a/6b**[b]
1						
3						
4				6.31, s	4.37, d (16.8)	4.39, d (16.7)
					4.11, d (16.8)	4.00, d (16.7)
5	7.90, br d (7.5)	7.90, br d (7.8)	8.06, br d (8.1)	7.38, br d (7.8)	7.29, br d (7.8)	7.27, br d (7.8)
6	7.87, m	7.86, m	7.84, m	7.70, td (7.5, 1.0)	7.47, t (7.5)	7.47, t (7.5)
7	7.58, m	7.58, m	7.57, m	7.50, td (7.5, 1.0)	7.33, t (7.5)	7.34, t (7.5)
8	8.23, br d (7.9)	8.22, br d (7.9)	8.22, br d (8.0)	8.28, br d (7.9)	7.99, br d (7.8)	8.00, br d (7.8)
9						
10						
1'	5.08, br s	5.03, br s	5.08, td (7.2, 1.6)	3.60, m	3.37, d	3.46, m
2'	2.11, td (13.8, 3.8)	2.03, dt (13.7, 2.7)	2.25, m	2.34, m	2.10, m	2.18, m
	1.81, dt (13.8, 2.4)	1.69, td (13.7, 3.6)	1.67, m	1.69, m	1.72, m	1.56, m
3'	2.65, m	2.53, m	2.29, m	2.29, m	2.62, m	2.23, m
4'	3.94, d (6.2)	3.45, d (10.5)	3.62, d (7.0)	3.07, d (12.1)	3.37, d (11.8)	3.42, d (12.0)
5'						
6'	2.75, qd (7.2, 2.3)	2.78, m	2.72, m	2.44, m	2.84, m	2.41, m
		2.58, m	2.64, m			
7'	1.06, t (7.2)	1.10, t (7.2)	1.08, t (7.2)	1.20, d (6.4)	1.13, d (6.7)	1.16, d (6.4)
8'	1.12, d (7.1)	1.07, d (6.7)	1.18, d (6.8)	1.08, d (6.3)	1.02, d (6.4)	1.01, d (6.1)
1"					4.29, q (7.1)	4.29, q (7.1)
2"					1.36, t (7.1)	1.36, t (7.1)

[a] Data were recorded in CD_3OD. [b] Data were recorded in $CDCl_3$.

Table 2 ^{13}C NMR data (150 MHz) for compounds**1** -**6** (δ in ppm, J in Hz).

No.	**1**[a]	**2**[a]	**3a/3b**[a]	**4a/4b**[b]	**5a/5b**[b]	**6a/6b**[b]
1	163.7, C	163.4, C	163.7, C	162.7, C	167.2, C	167.2, C
3	154.1 C	153.3, C	152.2, C	153.0, C	204.4, C	204.6, C
4	115.0, C	114.7, C	115.9, C	107.2, CH	48.8, CH_2	49.8, CH_2
5	124.8, CH	124.7, CH	126.4, CH	125.5, CH	132.7, CH	132.9, CH
6	136.5, CH	136.6, CH	136.1, CH	135.0, CH	132.2, CH	132.4, CH
7	129.4, CH	129.5, CH	129.4, CH	128.4, CH	127.1, CH	127.3, CH
8	130.6, CH	130.6, CH	130.4, CH	129.8, CH	130.6, CH	130.8, CH
9	138.3, C	138.3, C	138.2, C	137.0, C	136.2, C	136.2, C
10	122.0, C	121.9, C	122.1, C	120.7, C	130.0, C	129.9, C
1'	63.7, CH	63.5, CH	65.1, CH	73.9, CH	73.7, CH	74.1, CH
2'	37.0, CH_2	40.2, CH_2	39.5, CH_2	42.8, CH_2	40.4, CH_2	42.4, CH_2
3'	28.1, CH	28.6, CH	31.4, CH	30.8, CH	30.4, CH	29.9, CH
4'	55.0, CH	60.7, CH	59.4, CH	61.8, CH	69.4, CH	68.0, CH

No.	1[a]	2[a]	3a/3b[a]	4a/4b[b]	5a/5b[b]	6a/6b[b]
5'	212.0, C	212.1, C	211.8, C	205.1, C	208.5, C	207.5, C
6'	40.9, CH_2	37.1, CH_2	37.6, CH_2	53.5, CH	49.8, CH	53.9, CH
7'	7.7, CH_3	8.2, CH_3	8.1, CH_3	20.8, CH_3	20.5, CH_3	20.6, CH_3
8'	18.8, CH_3	19.9, CH_3	20.6, CH_3	10.6, CH_3	10.8, CH_3	10.4, CH_3
1"					60.9, CH_2	61.0, CH_2
2"					14.3, CH_3	14.4, CH_3

[a] Data were recorded in CD_3OD. [b] Data were recorded in $CDCl_3$.

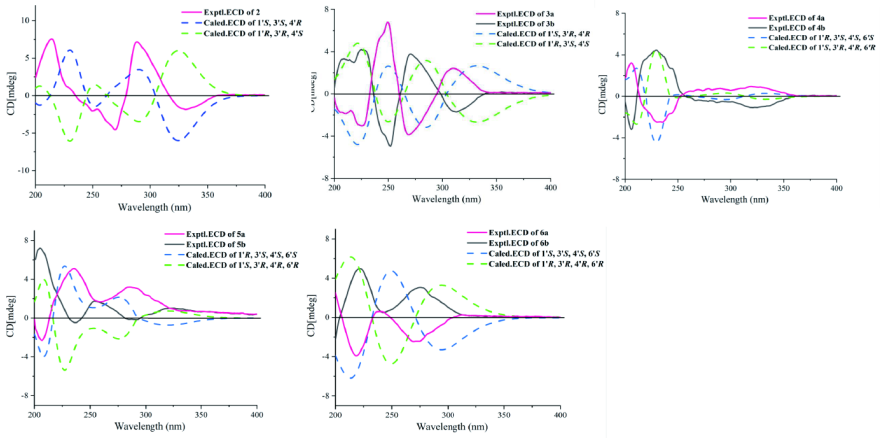

Figure 6 The experimental and calculated ECD spectra of compounds **2** -**6** .

Figure 7 Hypothetical biosynthetic pathways for compounds**1** -**6** .

indicating that it was a racemic mixture. Through chiral resolution, the enantiomers **6a** and **6b** were effectively separated, and their absolute configurations were established as 1'*S* ,3'*S* ,4'*S* ,6'*S* , and 1'*R* ,3'*R* ,4'*R* ,6'*R* by comparision of the experimental and calculated ECD spectra, respectively.

Compounds **1** , **2** , and **3a/3b** exhibit a unique 6/6/6-tricyclic system composed of an unusual fusion between a 1-(2-methylcyclohexyl) propan-1-one moiety and an isocoumarin core skeleton. Compounds **4a/4b** feature an unexpected scaffold of 2,5-dimethylcyclohexan-1-one, while compounds **5a/5b** and**6a/6b** represent rare examples of 1,2-*seco* -isocoumarin. Their biosynthetic pathways are speculated to originate from the naturally occurring isocoumarins (Figure 7).[7]The precursor of isocoumarin could band a single isopentenyl pyrophosphate (IPP) fragment to form intermediate **i** . Then, the oxidation reactions and intramolecular cyclization would generate**ii** with a six-membered ring, which further attaches a propionyl-CoA at the olefin position to form the compounds**1** -**3** , and compound **4** could be formed through ring cleavage and aldol condensation. Compound **4** was proposed to undergo intramolecular lactone ring cleavage and esterification reactions, resulting in the formation of compounds **5** and**6** .

Considering the similar chemical structures of compounds**1** -**6** , we initially selected compound **1** for preliminary mechanistic investigation *via* network pharmacological analysis. 110 genes were predicted as the potential targets of compound**1** by Swiss Target Prediction (Table S5). 148 DEGs (43 up- and 105 down-regulated) obtained in GEO datasets (Figure 9A) were aggregated with 537 HCC genes obtained in DisGeNET, GeneCards and TTD databases, and a total of 580 HCC genes were obtained. Among them, 24 genes were predicted as targets of compound **1** (Figures 9B-D), and eight of them, including CDK2, AURKA, CCNB1, CA9, CDK1, KDR, MKNK1, and MMP1 exhibited a significant correlation with HCC patient survival (Figure S70 and Figure 9E). GO and KEGG pathway enrichment analysis of above eight

candidates dispalyed that compound **1** was significantly enriched in regulation of cell cycle, kinase activity, MAPK signaling pathway, and PI3K-Akt signaling pathway (Figures 10A-B).

Subsequently, a molecular docking was performed to identify

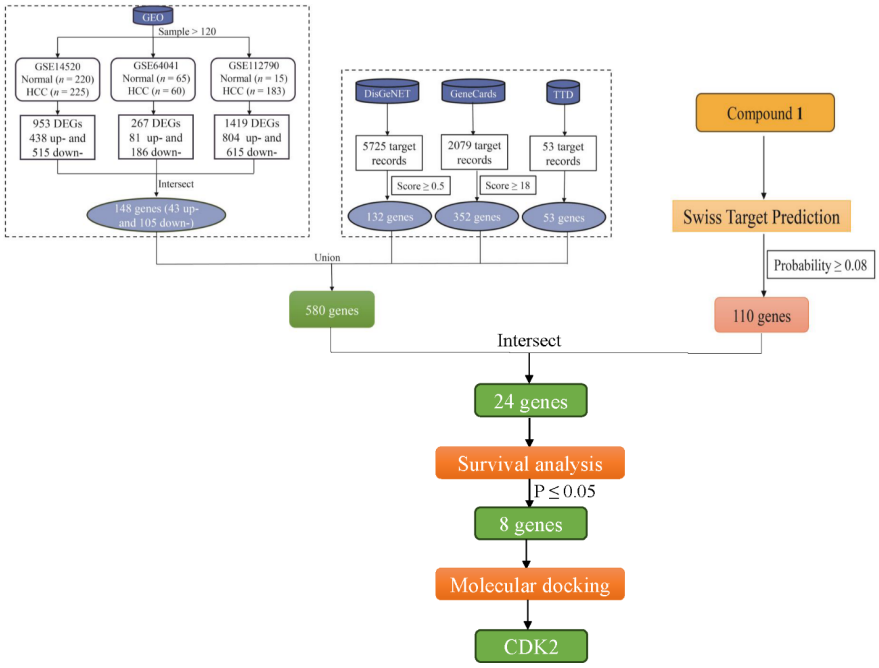

Figure 8 Flow chart of the target prediction of HCC and compound **1** by network pharmacological analysis.

the target of compound **1** among above eight candidates. As a result, compared to the others, compound **1** exhibited highest binding affinity with CDK2 (Figure S71 and Figure 11). In addition, CDK2 exhibited the good ability to distinguish HCC tumors from normal samples with the area under the Receiver Operating Characteristic (ROC) curve close to 0.8 (Figure 9F). These results suggested that CDK2 deeply involved in HCC progression[26-28] was a promising target of compound **1** , which might exert their inhibitory activity by targeting on CDK2.

In order to further validate the antihepatoma activities, compounds**1** -**6** were evaluated for their inhibitory activity on HepG2, Huh7, and SK-Hep-1 cell lines in *vitro* . As shown in Figure 12, compounds **1** and **2** exhibited antihepatoma activity on three cell lines with an inhibitory ratio of 85.1%, 84.5% (HepG2), 88.2%, 87.3% (Huh7) and 69.2%, 69.1% (SK-Hep-1) at 200 μ M, respectively.

Conclusions

In conclution, ten novel isocoumarins, artemdubones A-F, were isolated and identified from *A. dubia* var. *subdigitata* . Compounds**1** , **2** , and **3a/3b** possessed a unique 6/6/6-tricyclic system with an unprecedented 1-(2-methylcyclohexyl) propan-1-one moiety fused isocoumarin core skeleton, compounds**4a/4b** incorporated an unexpected 2,5-dimethylcyclohexan-1-one scaffold, and compounds **5a/5b** and **6a/6b** were a rare 1,2-*seco* -isocoumarin. Their structures including absolute configuration were elucidated *via* extensive spectral data, X-ray crystallography, and quantum chemical calculations. Network pharmacological analysis and molecular docking revealed that the targets of compound **1** were enriched in the cell cycle and PI3K-Akt signaling pathway, as well as in the targeting of the CDK2 protein. Compounds **1** and **2** showed inhibitory activity on three cell lines with an inhibitory ratio of 85.1% and 84.5% (HepG2), 88.2% and 87.3% (Huh7), and 69.2% and 69.1% (SK-Hep-1) at 200 μ M, respectively. Artemdubones A-F represented three new types of isocoumarins with unusual carbon skeletons from the genus*Artemisia* .

Experimental

General experimental procedures are provided in Supporting Information.

Plant materials

Artemisia dubia var. *subdigitata* samples were collected in June 2022 from Zhaotong City, Yunnan Province of China, and authenticated by Dr. Xiao-Lei Ma, from the Key Laboratory of Biodiversity and Biogeography, the Kunming Institute of Botany, Chinese Academy of Sciences. A voucher specimen (No. 20220630) has been deposited at the Laboratory of Antivirus and Natural Medicinal Chemistry, Kunming Institute of Botany, Chinese Academy of Sciences.

Extraction and isolation

The airdried aerial parts of *A . dubia* var.*subdigitata* (102 kg) were powdered and extracted two times with 90% ethanol at room temperature (each 800L). The combined extracts were concentrated under reduced pressure to yield a crude residue. The crude residue (9.6 kg) was then subjected to a silica gel column chromatography (Si CC) and eluted stepwise with a mixed solvent of acetone-petroleum ether (0:100, 10:90, 20:80, 30:70, 40:60

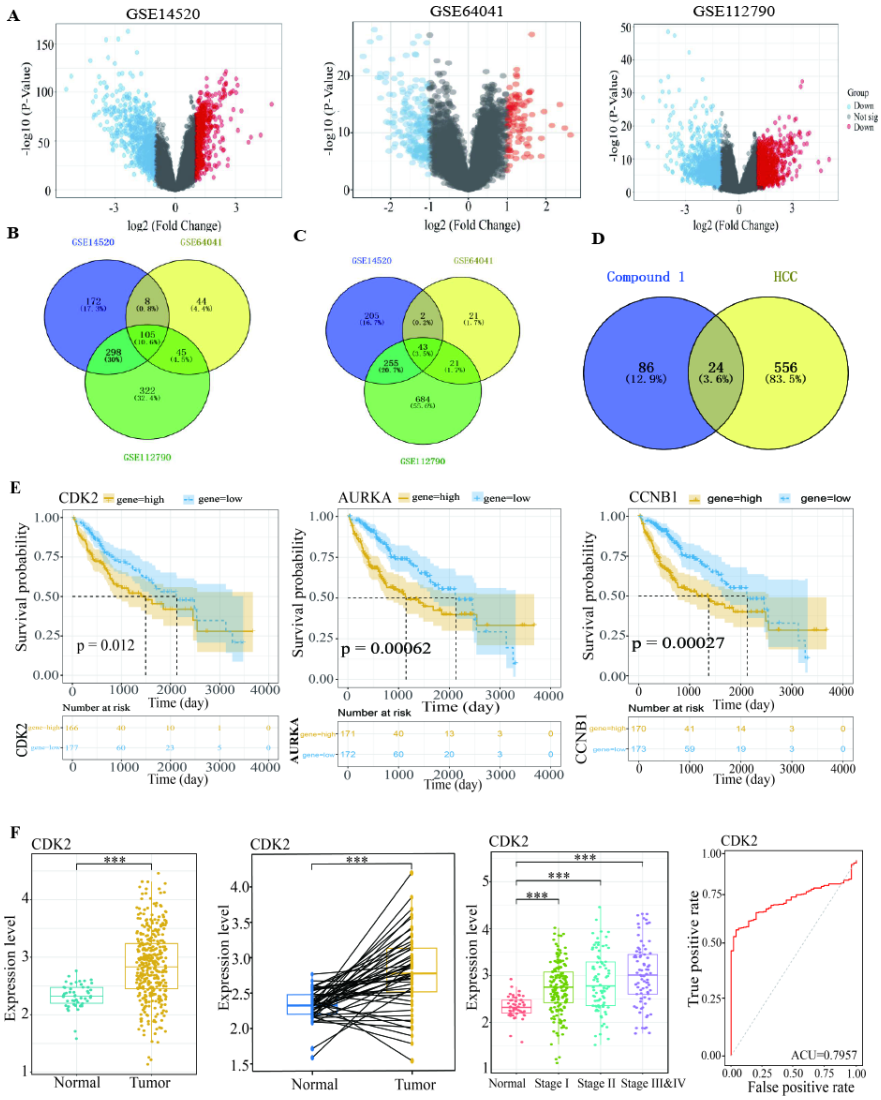

Figure 9 Results of target prediction and DEGs filtered. (A) Volcano maps of DEGs in GSE14520, GSE64041, and GSE112790. (B) The Venny results of low expression DEGs in HCC. (C) The Venny results of high expression DEGs in HCC. (D) The Venny results of potential target genes of compound **1** for HCC. (E) Survival curves of CDK2, AURKA, and CCNB1 in HCC patients using TCGA database. (F) The relative expression levels, survival rates, and ROC curves for CDK2 in LIHC using TCGA dataset.

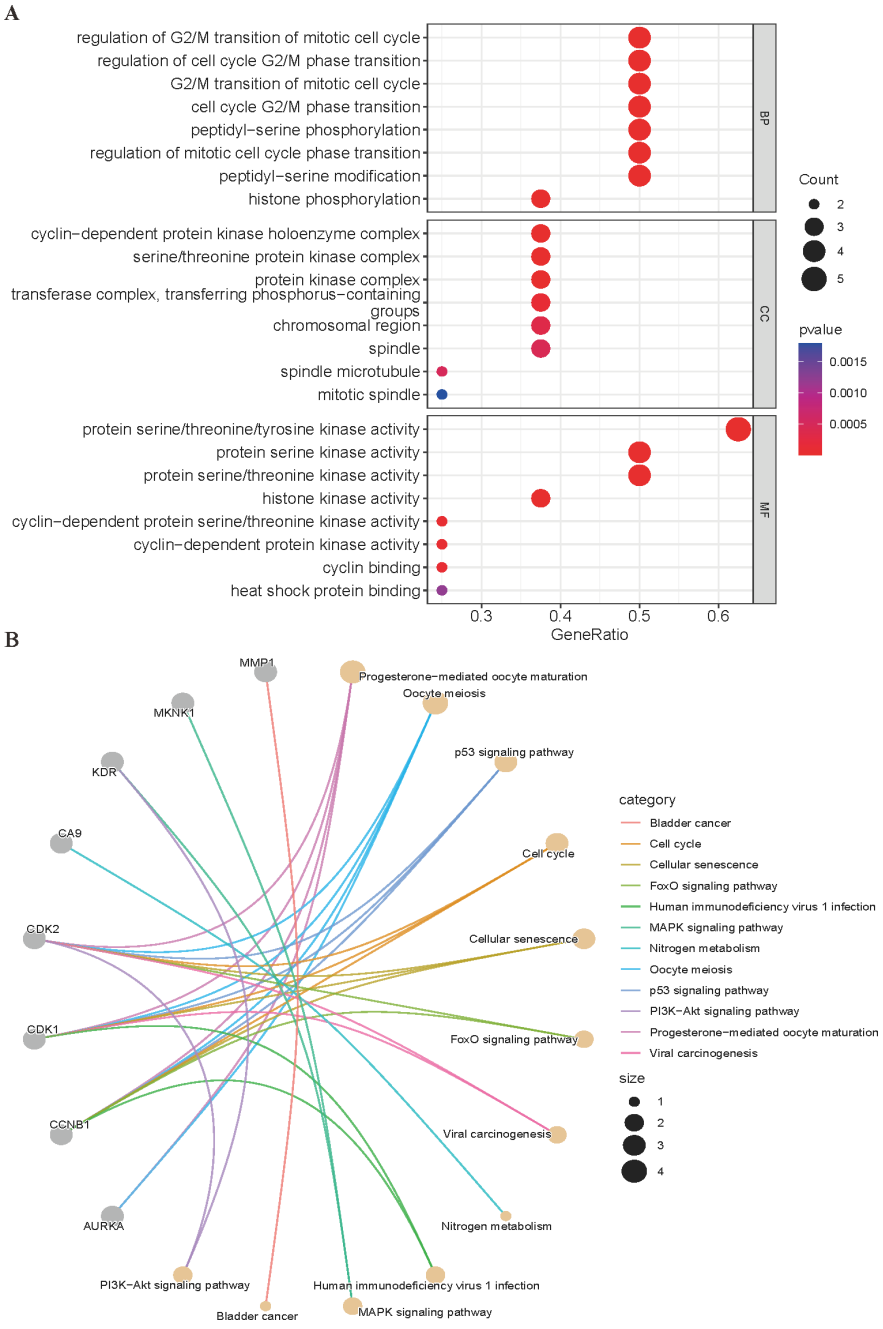

Figure 10 Results of enrichment analysis of the potential targets. (A) Go enrichment analysis of common targets. (B) KEGG enrichment analysis of common targets.

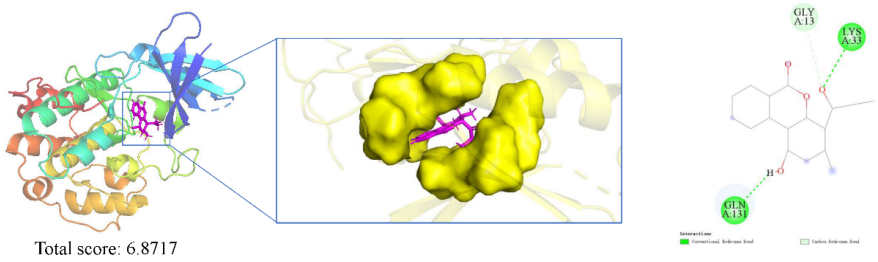

Figure 11 Binding capacity between compound **1** and CDK2 (PDB: 3NS9).

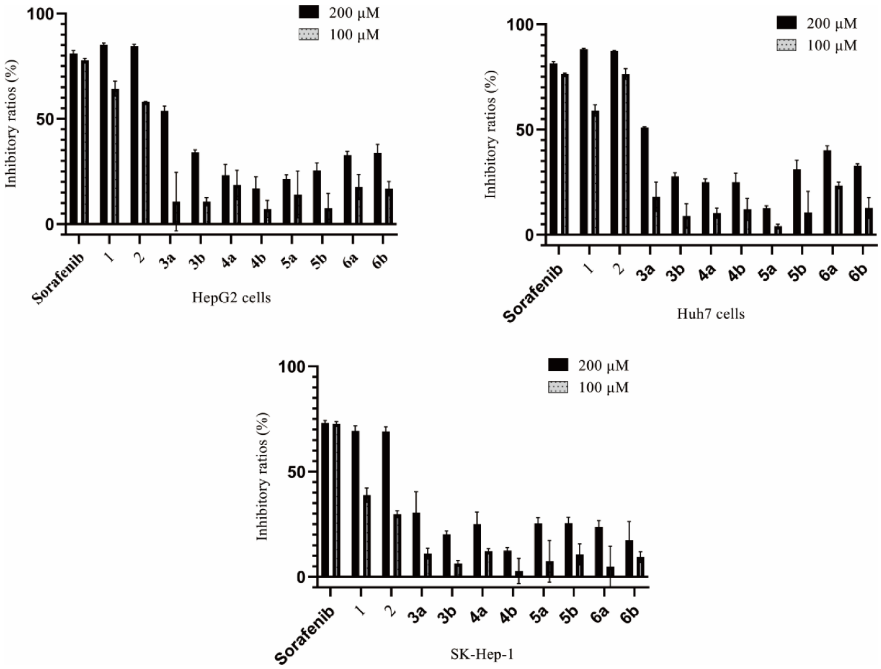

Figure 12 Antihepatoma activity of compounds**1** -**6** on HepG2, Huh7, and SK-Hep-1 cell lines at 200.0 and 100.0 μ M. Sorafenib was used as the positive control. Data were expressed as mean ± SD (n = 3).

and 50:50, *v/v*) to afford twelve fractions Frs. A-L. Fr. E (265 g) was subjected to MCI gel CHP 20P CC and eluted with the MeOH-H_2O system (50:50, 70:30, 90:10, 100:0) to yield four fractions (Frs. E-1-E-4). Fr. E-2 (26 g) was divided into five fractions (Frs. E-2a-E-2e) by Si CC (acetone-petroleum ether, 5: 95, 10:90, 20:80, 30:70). Fr. E-2d (3.4 g) was separated by Si CC eluted with acetone-$CHCl_3$ (20:80) to provide three fractions (Frs. E-2d-1-2d-3). Fr. E-2d-1(1.8 g) was fractionated by Sephadex LH-20 CC (MeOH-$CHCl_3$), Si CC (MeOH-$CHCl_3$, 5:95), and HPLC purification (Agilent XDB-C18 column, MeCN-H_2O, 36:64, 33:67) to yield compounds **1**(11 mg, t_R = 23.5 min), **2** (5 mg,t_R = 27.0 min) and **3** (11 mg,t_R = 35.4 min). Fr. E-2d-2(1.2 g) was repeatedly purified by Rp-C_{18} CC (MeOH-H_2O, 30:70, 50:50, 60:40, 70:30), Si CC (MeOH-$CHCl_3$, 2:98 to 10:90), and HPLC (MeCN-H_2O, 45:55) to afford compounds**4** (9 mg, t_R = 24.0 min), **5** (14 mg, t_R = 27.4 min), **6** (17 mg,t_R = 32.5 min).

The compounds **3** -**6** were performed on an Opti-Chiral(r)C1-5 column (MeCN-H_2O, 19:81 for **3** ; 15:85 for **4** ; MeOH-H_2O, 52:48 for **5** ; 56:44 for **6**) to yield the enantiomers **3a** (4 mg,t_R = 22.5 min), **3b** (4 mg,t_R = 25.0 min), **4a** (3 mg,t_R = 14.0 min), **4b** (3 mg,t_R = 17.0 min), **5a** (5 mg,t_R = 19.0 min), **5b** (5 mg,t_R = 21.5 min), **6a** (7 mg,t_R = 26.0 min), **6b** (7 mg,t_R = 28.5 min).

*Artemdubone A (**1**)* : White triclinic crystals (MeOH–$CHCl_3$, 15:85); mp 178-180 ; $[\alpha]_D^{23}$ -15.0 (*c* 0.040, MeOH); UV (MeOH) λ_{max} (log ϵ): 231 (3.54) nm; ECD (MeOH) λ_{max} ($\Delta\epsilon$) 265 (+1.08), 289 (–0.32) nm; IR v_{max} 3445, 1716, 1656, 1459, 1315, 1075, 779 cm^{-1}; ^1H and^{13}C NMR data see Tables 1 and 2; (–)-HRESIMS*m /z* 285.1162 ($[M - H]^-$ (calcd. for $C_{17}H_{17}O_4$, 285.1149).

*Artemdubone B (**2**)* : White powers; $[\alpha]_D^{23}$ +16.9 (*c*0.071, MeOH); UV (MeOH) λ_{max} (log ϵ): 230 (3.80) nm; ECD (MeOH) λ_{max} ($\Delta\epsilon$) 210 (+14.60), 264 (–8.78) nm; IR v_{max} 3446, 1719, 1653, 1457, 1383, 1028, 977, 697 cm^{-1};^1H NMR and ^{13}C NMR data see Tables 1 and 2; (+)-HRESIMS *m/z* 287.1266 ($[M + H]^+$(calcd. for $C_{17}H_{19}O_4$, 287.1278).

*Artemdubone C (**3**)* : White powers; UV (MeOH)λ_{max} (log ϵ): 231 (3.45) nm; IRv_{max} 3447, 1718, 1653, 1457, 1383, 1028, 779 cm^{-1}; ^1H NMR and^{13}C NMR data see Tables 1 and 2; (+)-HRESIMS*m/z* 309.1115 ($[M + Na]^+$ (calcd. for $C_{17}H_{18}O_4Na$, 309.1097).

*(+)-Artemdubone C (**3a**)* : $[\alpha]_D^{23}$ +27.1 (*c* 0.038, MeOH); ECD (MeOH) λ_{max} ($\Delta\epsilon$) 239 (–2.73), 264 (+6.20), 283 (–7.01), 323 (+2.17) nm.

*(-)-Artemdubone C (**3b**)* : $[\alpha]_D^{23}$ –40.7 (*c* 0.041, MeOH); ECD (MeOH) λ_{max} ($\Delta\epsilon$) 237 (+3.53), 264 (–4.15), 284 (+6.36), 325 (–1.43) nm.

*Artemdubone D (**4**)* : Colorless triclinic crystals (MeOH–$CHCl_3$, 30:70); mp 176-181 ; UV (MeOH)λ_{max} (log ϵ): 229 (2.67) nm; IRv_{max} 3517, 1720, 1693, 1601, 1451, 1300, 1030, 721 cm^{-1}; ^1H NMR and^{13}C NMR data see Tables 1 and 2; (+)-HRESIMS*m/z* 287.1262 ($[M + H]^+$ (calcd. for $C_{17}H_{19}O_4$, 287.1278).

*(+)-Artemdubone D (**4a**)* : $[\alpha]_D^{20}$ +11.3 (*c* 0.031, MeOH); ECD (MeOH) λ_{max} ($\Delta\epsilon$) 200 (+0.89), 228 (–0.69), 313 (+0.26) nm.

*(-)-Artemdubone D (**4b**)* : $[\alpha]_D^{21}$ –11.6 (*c* 0.035, MeOH); ECD (MeOH) λ_{max} ($\Delta\epsilon$) 201 (–0.79), 225 (+1.10), 316 (–0.27) nm.

*Artemdubone E (**5**)* : White powers; UV (MeOH)λ_{max} (log ϵ): 197 (3.27) nm; IRv_{max} 3441, 1718, 1633, 1606, 1451, 1266, 1030, 724 cm^{-1}; ^1H NMR and^{13}C NMR data see Tables 1 and 2; (+)-HRESIMS*m/z* 355.1524 ($[M + Na]^+$ (calcd. for $C_{19}H_{24}O_5$, 355.1516).

*(+)-Artemdubone E (**5a**)* : $[\alpha]_D^{20}$ +31.4 (*c* 0.032, MeOH); ECD (MeOH) λ_{max} ($\Delta\epsilon$) 202 (–1.37), 232 (+2.97), 249 (+1.03), 280 (+1.88) nm.

*(-)-Artemdubone E (**5b**)* : $[\alpha]_D^{21}$ –25.2 (*c* 0.034, MeOH); ECD (MeOH) λ_{max} ($\Delta\epsilon$) 201 (+4.24), 230 (–0.25), 250 (+1.01), 280 (–0.09) nm.

*Artemdubone F (**6**)* : White powers; UV (MeOH)λ_{max} (log ϵ): 198 (3.59) nm; IRv_{max} 3464, 1723, 1689, 1602, 1302, 1275, 1032, 723 cm^{-1}; ^1H NMR and^{13}C NMR data see Tables 1 and 2; (+)-HRESIMS*m/z* 355.1527 ($[M + Na]^+$ (calcd. for $C_{19}H_{24}O_5$, 355.1516).

*(+)-Artemdubone F (**6a**)* : $[\alpha]_D^{21}$ +50.1 (*c* 0.040, MeOH); ECD (MeOH) λ_{max} ($\Delta\epsilon$) 201 (–9.76), 230 (+6.25), 251 (+0.63), 285 (+3.86) nm.

*(-)-Artemdubone F (**6b**)* : $[\alpha]_D^{21}$ –61.9 (*c* 0.048, MeOH); ECD (MeOH) λ_{max} ($\Delta\epsilon$) 200 (+10.65), 230 (–4.10), 250 (+0.63), 284 (–2.53) nm.

X-ray crystallographic analyses

Compounds **1** and **4** were obtained by recrystallization in a mixture of MeOH-$CHCl_3$ (15:85) and MeOH-$CHCl_3$ (30:70), respectively. X-ray diffraction data were recorded on a Bruker D8 QUEST instrument using Cu K*α*radiation. The structures of two compounds were determined using direct methods (SHELXS97), and difference Fournier techniques and refined by full-matrix least squares calculations. The nonhydrogen

atoms were refined anisotropically, and hydrogen atoms were determined at calculated positions. The crystallographic data of those compounds were deposited at the Cambridge Crystallographic Data Centre (**1** : CCDC 2330652; **4** : 2330657).

Crystal data for compound **1** . $C_{17}H_{18}O_4$, $M = 286.31$, $a = 10.3468(4)$ Å, $b = 8.1059(3)$ Å, $c = 17.3732(7)$ Å, $\alpha = 90°$, $\beta = 90°$, $\gamma = 90°$, $V = 1457.09(10)$ Å^3, $T = 150.(2)$ K, space group*Pna* 21, $Z = 4$, μ (Cu Kα) = 0.757 mm^{-1}, 18925 measured reflections, 2770 independent reflections ($R_{int} = 0.1259$). The finalR_1 values were 0.0428 ($I > 2\sigma$ (I)). The final wR (F^2) values were 0.1107 ($I > 2\sigma$ (I)). The final R_1 values were 0.0489 (all data). The finalwR (F^2) values were 0.1157 (all data). The goodness of fit on F^2 was 1.122. Flack parameter = 0.22(17).

Crystal data for compound **4** . $C_{17}H_{18}O_4$, $M = 286.31$, $a = 15.3594(9)$ Å, $b = 10.1798(6)$ Å, $c = 18.3134(11)$ Å, $\alpha = 90°$, $\beta = 100.679(2)°$, $\gamma = 90°$,$V = 2813.8(3)$ Å^3, $T = 150.(2)$ K, space group P 121/c 1, $Z = 8$, μ (Cu Kα) = 0.784 mm^{-1}, 30313 measured reflections, 5135 independent reflections ($R_{int} = 0.1603$). The finalR_1 values were 0.1157 ($I > 2\sigma$ (I)). The final wR (F^2) values were 0.2819 ($I > 2\sigma$ (I)). The final R_1 values were 0.1399 (all data). The finalwR (F^2) values were 0.3043 (all data). The goodness of fit on F^2 was 1.188.

Quantum chemistry calculation

Conformational searches for C**-** 1'S * and C**-** 1'R * in **2** were conducted with MMFF94 force field by SPARTAN software.[29] These conformers were subjected to DFT geometry optimization at the B3LYP/6-31G(d) on the Gaussian 09 program. Frequency analyses of all optimized conformers were conducted with the same level of theory to ensure that no imaginary frequency existed. Then, thermal corrections to Gibbs free energies obtained by frequency analyses were added to the M062X/6-311+G(2d,p) level to get the Gibbs free energies of each conformer. Subsequently, room-temperature (298.15 K) equilibrium populations were calculated according to the Boltzmann distribution low.[30]Those conformers with a population of over 2% were subjected to subsequent NMR calculations. NMR shielding constants of compound**2** were calculated with the gauge-including atomic orbital (GIAO) method at the mPW1PW91-SCRF/6-31 + G(d,p) level and based on the procedure described in a previous report.[31] The linear correlation coefficient (R^2), the mean absolute error (MAE), the corrected mean absolute error (CMAE) and custom DP4+ probability were calculated to evaluate deviations between the experimental and calculated results. [24] The theoretical ECD calculations of the conformations of compounds were performed by means of TDDFT methodology at the B3LYP/6-311+G(d,p) level with the consideration of solvent effects. The overall calculated ECD curves were generated by using SpecDis 1.71.[32]

Target prediction of compound 1

Compound **1** was screened using the SwissADME program (*http://swissadme.ch/index.php/*),[33]which includes assessments of gastrointestinal absorption (GI absorption) and drug-likeness (Lipinski, Ghose, Veber, Egan, Mugge). Swiss Target Prediction database (*http://swisstargetprediction.ch/*)[34]was used to predict the targets of compound **1** , and the targets with probability [?] 0.08 in the prediction results were selected for further analysis.

The gene expression profile of 468 HCC samples and 300 normal samples were obtained from Gene Expression Omnibus database (GEO, https://portal. gdc.cancer.gov/) with the accession number of GSE14520, GSE64041 and GSE112790. The differential expression genes (DEGs) were achieved using GEO-query and limma R packages, and which were integrated and visualized with volcano map (p ¡0.05 and $|\log_2 FC|$¿1). Liver hepatocellular carcinoma (LIHC) of The Cancer Genome Atlas (TCGA,*https://portal.gdc.cancer.gov/*) was used for further analysis. Survival analysis and ROC curves were performed using the R package. HCC genes were collected from DisGeNET (*https://www.disgenet.org/*), GeneCards (*https://www.genecards.org/*) and TTD (*https://db.idrblab.net/ttd/*). The framework for target generation was shown in Figure 8.

The common targets were obtained by intersecting the targets of the compound **1** with HCC genes. The Gene Ontology (GO) and Kyoto Encyclopedia of Genes and Genomes (KEGG) were analyzed using clusterProfiler

package in the R software.

Molecular docking

The molecular docking study was conducted by Sybyl-X 2.1.1, and the crystal structure of the CDK2 protein (PDB: 3NS9) was obtained from the RCSB Protein Data Bank (*http://www.wwpdb.org*). All polar hydrogen atoms were added. Prior to the docking process, the substructures of the ligands were extracted, and water molecules were eliminated. The surflex-dock total score was expressed as -logK_{d} to indicate binding affinities, where a higher docking total score corresponds to a stronger interaction between protein and compound.

Bioactivity assays

Compounds **1** -**6** were tested for their antihepatoma activity on three human hepatoma cell lines (HepG2, Huh7 and SK-Hep-1) by the MTT method. The cells with a density of 1×10^4cells/well of media were seeded in a 96-well plate and incubated for 24-hour with 5% CO_2 at 37 °C and were treated with 100μ L of culture medium which contained different concentrations of compounds and incubated for 48 hours. At the end of exposure time and removal of all the medium in the wells, 100 μ L of MTT solution (1 mg/mL) was added into each well and the plates were incubated in the dark for 4 hours at 37 °C. Afterward, the remained liquid was removed, and the MTT formazan crystals were dissolved in 100 μ L of dimethyl sulfoxide (DMSO). Then, the absorbance was measured at 490 nm using a microplate reader from BIO-RAD (USA). The inhibitory ratios were calculated as (1 - $A_{490\mathrm{treated}}/A_{490\ \mathrm{control}}$) × 100%.

Supporting Information

The supporting information for this article is available on the WWW under https://doi.org/10.1002/cjoc.202400xxx.

Acknowledgement

This work was financially supported by the Key Program of the National Natural Science Foundation of China (22137008), the Xingdian Yingcai Project (YNWR-KJLJ-2019-002), the Youth Innovation Promotion Association, CAS (2020386), and the Reserve Talents of Young and Middle-aged Academic and Technical Leaders in Yunnan Province (202105AC160021).

References

1. Llovet, J. M.; Kelley, R. K.; Villanueva, A.; Singal, A. G.; Pikarsky, E.; Roayaie, S.; Lencioni, R.; Koike, K.; Zucman-Rossi, J.; Finn, R. S. Hepatocellular carcinoma. *Nat. Rev. Dis. Primers* .**2021** , *7* (1), 6.
2. Sung, H.; Ferlay, J.; Siegel, R. L.; Laversanne, M.; Soerjomataram, I.; Jemal, A.; Bray, F. Global cancer statistics 2020: GLOBOCAN estimates of incidence and mortality worldwide for 36 cancers in 185 countries. *CA. A. Cancer. J. Clin.* **2021** , *71*(3), 209–249.
3. Alawyia, B.; Constantinou, C. Hepatocellular Carcinoma: a narrative review on current knowledge and future prospects. *Curr. Treat. Options. Oncol.* **2023** , *24* (7), 711–724.
4. Luo, X. T.; He, X.; Zhang, X. M.; Zhao, X. H.; Zhang, Y. Z.; Shi, Y. S.; Hua, S.N. Hepatocellular carcinoma: signaling pathways, targeted therapy, and immunotherapy. *MedComm* . **2024** ; *5* , e474.
5. Jiang, L.; Li, L.; Liu, Y.; Zhan, M.; Lu, L.; Yuan, S.; Liu, Y. Drug resistance mechanism of kinase inhibitors in the treatment of hepatocellular carcinoma. *Front. Pharmacol.* **2023** ,*14* , 1097277
6. Taskforce; Atanasov, A. G.; Zotchev, S. B.; Dirsch, V. M.; Supuran, C. T. Natural products in drug discovery: advances and opportunities.*Nat. Rev. Drug. Discov.* **2021** , *20* (3), 200–216.
7. Saeed, A. Isocoumarins, miraculous natural products blessed with diverse pharmacological activities. *Eur. J. Med. Chem.***2016** , *116* , 290–317.
8. Shabir, G.; Saeed, A.; El-Seedi, H. R. Natural isocoumarins: structural styles and biological activities, the revelations carry on .... *Phytochemistry* **2021** , *181* , 112568.
9. Tammam, M. A.; Gamal El-Din, M. I.; Abood, A.; El-Demerdash, A. Recent advances in the discovery, biosynthesis, and therapeutic potential of isocoumarins derived from fungi: a comprehensive update. *RSC. Adv.* **2023** , *13* (12), 8049–8089.

10. Chaudhary, N. K.; Pitt, J. I.; Lacey, E.; Crombie, A.; Vuong, D.; Piggott, A. M.; Karuso, P. Banksialactones and banksiamarins: isochromanones and isocoumarins from an Australian fungus,*Aspergillus banksianus* . *J. Nat. Prod.* **2018** ,*81* (7), 1517–1526.
11. Kumar, J. S.; Thirupataiah, B.; Medishetti, R.; Ray, A.; Bele, S. D.; Hossain, K. A.; Reddy, G. S.; Edwin, R. K.; Joseph, A.; Kumar, N.; Shenoy, G. G.; Rao, C. M.; Pal, M. Rosuvastatin based novel 3-substituted isocoumarins/3alkylidenephthalides: ultrasound assisted synthesis and identification of new anticancer agents. *Eur. J. Med. Chem.* **2020** , *201* , 112335.
12. Park, M. J.; Kang, Y.-H. Isolation of isocoumarins and flavonoids as α-glucosidase inhibitors from *Agrimonia pilosa* L.*Molecules* **2020** , *25* (11), 2572.
13. Chen, C.; Ye, G. T.; Tang, J.; Li, J. L.; Liu, W. B.; Wu, L.; Long, Y. H. New polyke-tides from mangrove endophytic fungus *Penicillium*Sp. BJR-P2 and their anti-inflammatory activity. *Mar. Drugs* .**2022** , *20* (9), 583.
14. Su, L. H.; Zhang, X.; Ma, Y. B.; Geng, C. A.; Huang, X. Y.; Hu, J.; Li, T. Z; Tang, S.; Shen, C.; Gao, Z.; Zhang, X. M; Chen, J. J. New guaiane-type sesquiterpenoid dimers from *Artemisia atrovirens*and their antihepatoma activity. *Acta Pharmaceutica Sinica B***2021** , *11* (6), 1648–1666.
15. Feng, X.; Cao, S.; Qiu, F.; Zhang, B. Traditional application and modern pharmacological research of *Artemisia annua* L.*Pharmacol. Therapeut.* **2020** , *216* , 107650.
16. He, X. F.; Ma, W. J.; Hu, J.; Li, T. Z.; Geng, C. A.; Ma, Y. B.; Wang, M. F.; Yang, K. X.; Zhang, X. M.; Chen, J. J. Diverse structures and antihepatoma effect of sesquiterpenoid dimers from *Artemisia eriopoda* by AKT/STAT signaling pathway. *Signal. Transduct. Target. Ther.* **2023** , *8* (1), 64.
17. Li, K. M.; Dong, X.; Ma, Y. N.; Wu, Z. H.; Yan, Y. M.; Cheng, Y. X. Antifungal coumarins and lignans from *Artemisia annua* .*Fitoterapia* **2019** , *134* , 323–328.
18. Bhutia, T. D.; Valant-Vetschera, K. M. Chemodiversity of*Artemisia dracunculus* L. from Kyrgyzstan: isocoumarins, coumarins, and flavonoids from aerial parts. *Nat. Prod. Commun.***2008** , *3* (8), 1289-1292.
19. Mallabaev, A.; Sidyakin, G. P. Artemidiol — a new isocoumarin from*Artemisia dracunculus* . *Chem. Nat. Compd* . **1974** ,*10* (6), 743–745.
20. Greger, H. Aromatic acetylenes and dehydrofalcarinone derivatives within the *Artemisia dracunculus* group. *Phytochemistry***1979** , *18* (8), 1319-1322.
21. Lutz-Kutschera, G.; Engelmeier, D.; Hadacek, F.; Werner, A.; Greger, H.; Hofer, O. Synthesis of side chain substituted 3-butylisocoumarins and absolute configurations of natural isocoumarins from*Artemisia dracunculus* . *Monatsh. Chem.* **2003** ,*134* (9), 1195–1206.
22. Gao, Z.; Ma, W. J.; Li, T. Z.; Ma, Y. B.; Hu, J.; Huang, X. Y.; Geng, C. A.; He, X. F.; Zhang, X. M.; Chen, J. J. Artemidubolides A-T, cytotoxic unreported guaiane-type sesquiterpenoid dimers against three hepatoma cell lines from *Artemisia dubia* . *Phytochemistry***2022** , *202* , 113299.
23. Gu, W.; Wang, W.; Li, X. N.; Zhang, Y.; Wang, L. P.; Yuan, C. M.; Huang, L. J.; Hao, X. J. A novel isocoumarin with anti-influenza virus activity from *Strobilanthes cusia* . *Fitoterapia***2015** , *107* , 60–62.
24. Grimblat, N.; Zanardi, M. M.; Sarotti, A. M. Beyond DP4: an improved probability for the stereochemical assignment of isomeric compounds using quantum chemical calculations of NMR shifts. *J. Org. Chem.* **2015** , *80* (24), 12526–12534.
25. Xu, L.; Guo, F. W.; Zhang, X. Q.; Zhou, T. Y.; Wang, C. J.; Wei, M. Y.; Gu, Y. C.; Wang, C. Y.; Shao, C. L. Discovery, total syntheses and potent anti-inflammatory activity of pyrrolinone-fused benzoazepine alkaloids asperazepanones A and B from *Aspergillus candidus* .*Commun. Chem.* **2022** , *5* (1), 80.
26. Haider, C.; Grubinger, M.; Řezníčková, E.; Weiss, T. S.; Rotheneder, H.; Miklos, W.; Berger, W.; Jorda, R.; Zatloukal, M.; Gucký, T.; Strnad, M.; Kryštof, V.; Mikulits, W. Novel inhibitors of cyclin-dependent kinases combat hepatocellular carcinoma without inducing chemoresistance. *Mol. Cancer. Ther* . **2013** ,*12* (10), 1947–1957.
27. Sonntag, R.; Giebeler, N.; Nevzorova, Y. A.; Bangen, J. M.; Fahrenkamp, D.; Lambertz, D.; Haas, U.; Hu, W.; Gassler, N.; Cubero, F. J.; Müller-Newen, G.; Abdallah, A. T.; Weiskirchen, R.; Ticconi,

F.; Costa, I. G.; Barbacid, M.; Trautwein, C.; Liedtke, C. Cyclin E1 and cyclin-dependent kinase 2 are critical for initiation, but not for progression of hepatocellular carcinoma. *Proc. Natl. Acad. Sci. U.S.A.* **2018** , *115* (37), 9282–9287.

28. Farasati Far, B.; Rabie, D.; Hemati, P.; Fooladpanjeh, P.; Faal Hamedanchi, N.; Broomand Lomer, N.; Karimi Rouzbahani, A.; Naimi-Jamal, M. R. Unresectable hepatocellular carcinoma: a review of new advances with focus on targeted therapy and immunotherapy.*Livers* **2023** , *3* (1), 121–160.
29. Alden, K.; Read, M.; Timmis, J.; Andrews, P. S.; Veiga-Fernandes, H.; Coles, M. Spartan: A comprehensive tool for understanding uncertainty in simulations of biological systems. *PLoS. Comput. Biol.***2013** , *9* (2), e1002916.
30. Zu, W. Y.; Tang, J. W.; Hu, K.; Zhou, Y. F.; Gou, L. L.; Su, X. Z.; Lei, X.; Sun, H. D.; Puno, P.T. Chaetolactam A, an azaphilone derivative from the endophytic fungus *Chaetomium* sp. g1.*J. Org. Chem.* **2021** , *86* (1), 475–483.
31. Willoughby, P. H.; Jansma, M. J.; Hoye, T. R. A guide to small-molecule structure assignment through computation of (^{1}H and ^{13}C) NMR chemical shifts.*Nat. Protoc.* **2014** , *9* (3), 643–660.
32. Su, L. H.; Geng, C. A.; Li, T. Z.; Ma, Y. B.; Huang, X. Y.; Zhang, X. M.; Chen, J. J. Artatrovirenols A and B: two cagelike sesquiterpenoids from *Artemisia atrovirens* . *J. Org. Chem.* **2020** ,*85* (21), 13466–13471.
33. Daina, A.; Michielin, O.; Zoete, V. SwissADME: A free web tool to evaluate pharmacokinetics, drug-likeness and medicinal chemistry friendliness of small molecules. *Sci. Rep.* **2017** ,*7* (1), 42717.
34. Gfeller, D.; Grosdidier, A.; Wirth, M.; Daina, A.; Michielin, O.; Zoete, V. SwissTargetPrediction: a web server for target prediction of bioactive small molecules. *Nucleic. Acids. Res.* **2014** ,*42* (W1), W32–W38.

Manuscript received: XXXX, 2024 Manuscript revised: XXXX, 2024 Manuscript accepted: XXXX, 2024 Version of record c

The Authors

You will be invited to submit a most recent group photo with all the authors upon acceptance of the manuscript
Left to Right: Authors Names

Entry for the Table of Contents

Three Types of Isocoumarins with Unusual Carbon Skeletons from *Artemisia dubia* var. *subdigitata* and Th
Artemdubones A-F (**1**-**6**) were isolated from *Artemisia dubia* var. *subdigitata*. Compounds **1**, **2** and **3a**/**3b** possessed a unic

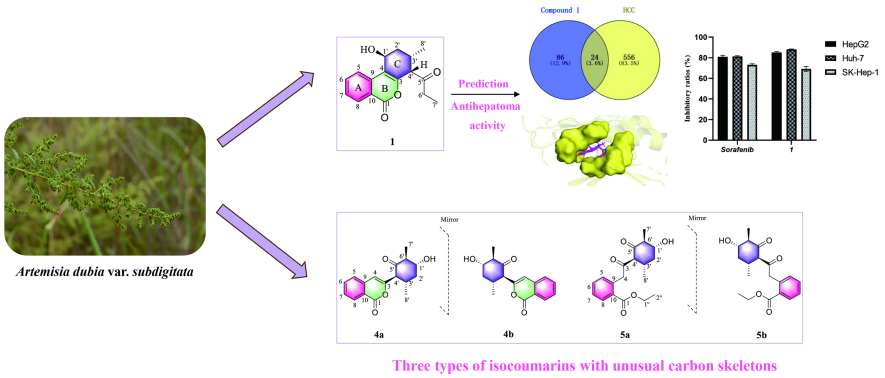

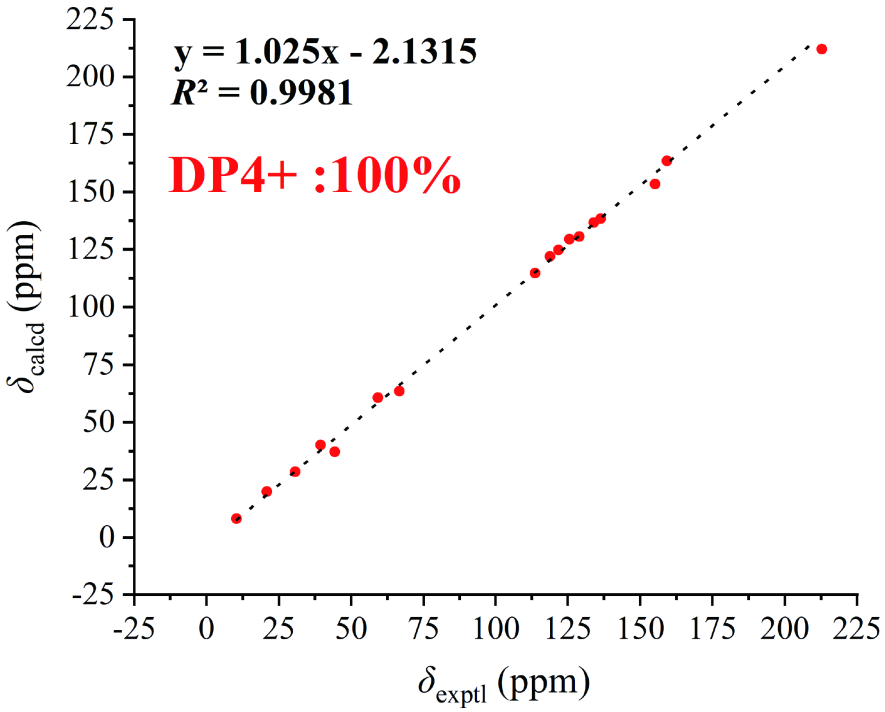

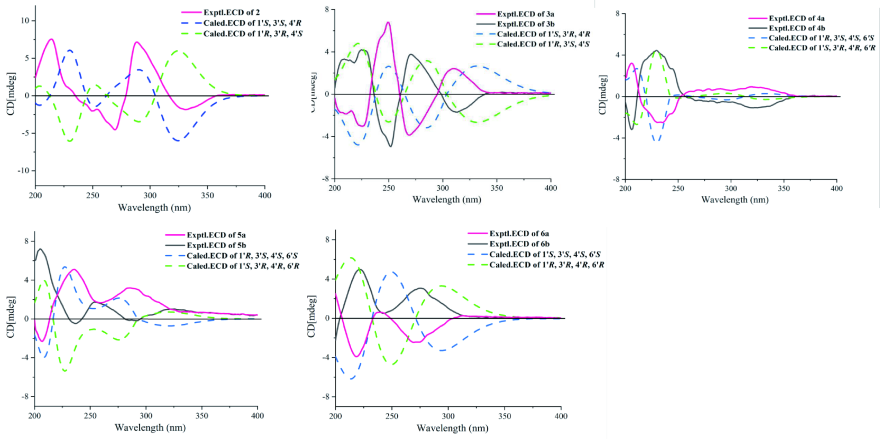

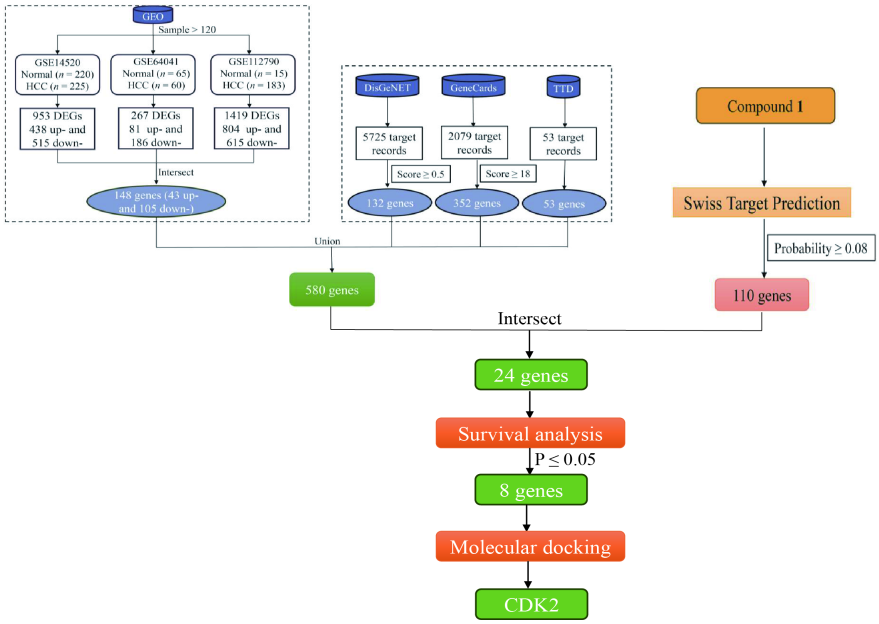

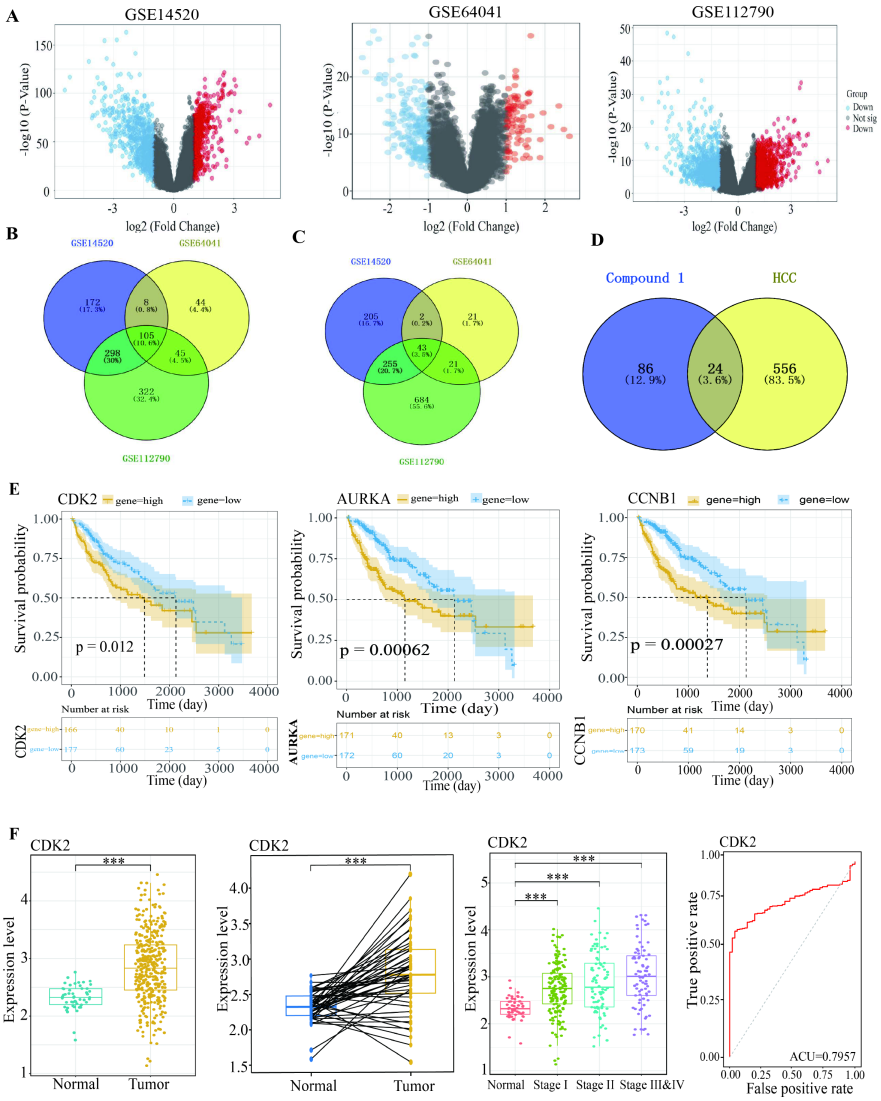

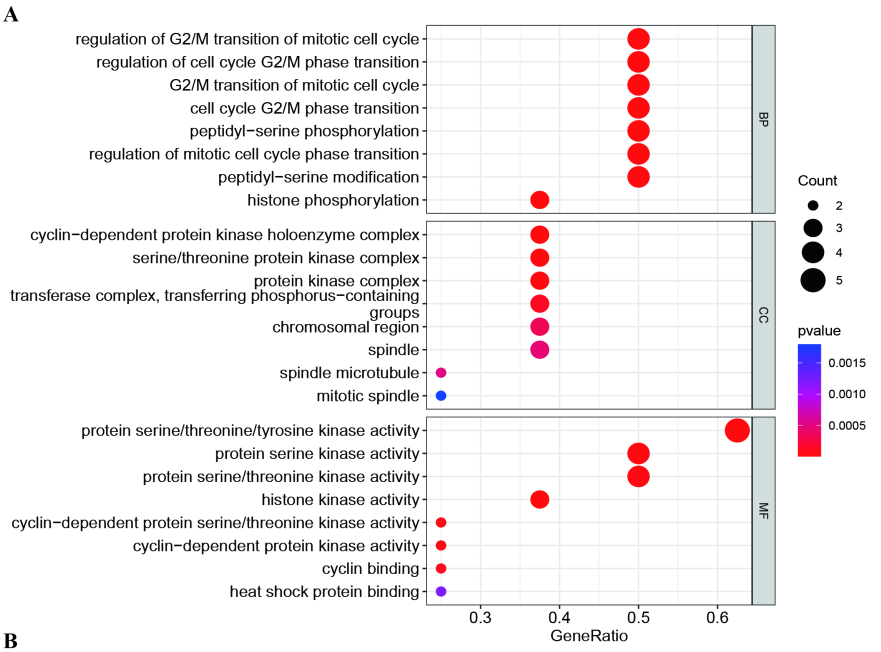

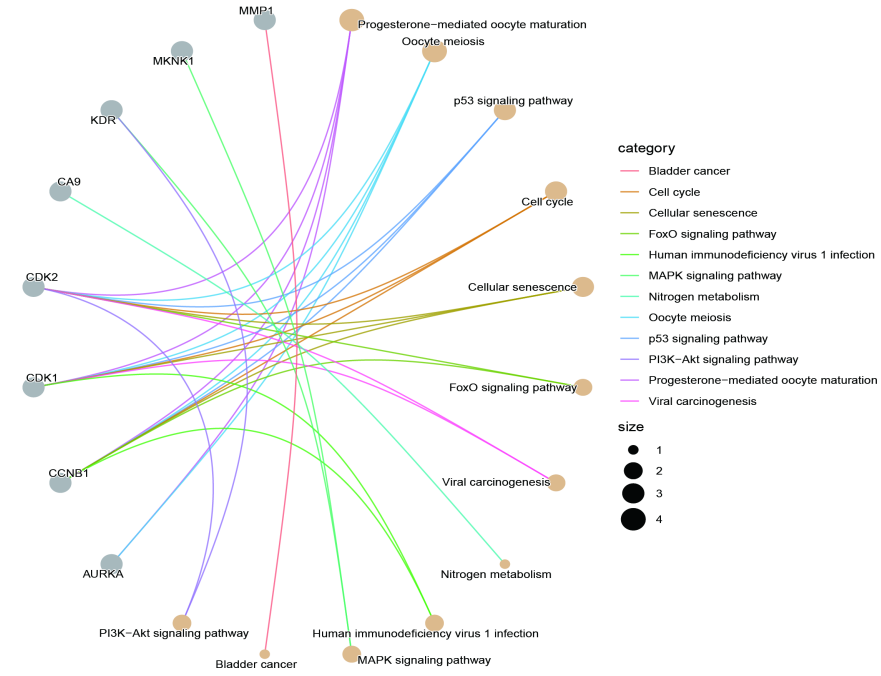

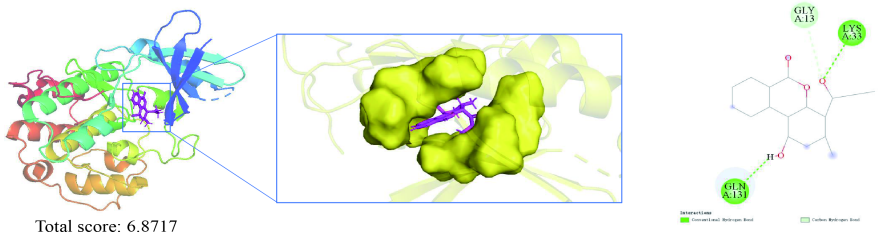

Total score: 6.8717